



CHAPTER II

LITERATURE REVIEW

2.1 Hydrogen: Fuel of the Future

Hydrogen is now being considered as an ideal fuel for the future. Hydrogen fuel can be produced from clean and renewable energy sources, and thus, life cycle of hydrogen is clean and renewable. However, presently, renewable energy contributes only about 5% of the commercial hydrogen production primarily via water electrolysis, while other 95% hydrogen is mainly derived from fossil fuels (Bak *et al.*, 2002). Hydrogen is one of the most important chemicals in the industrial commodity; it is mainly consumed in the hydrotreating and synthesis of ammonia, methanol, higher alcohols and aldehydes process. Moreover, hydrogen use for the powering of non-polluting vehicles, domestic heating, and aircraft. Therefore, hydrogen, as an energy carrier, is anticipated to join photovoltaic electricity as the foundation of sustainable energy system. Recent efforts in the development of vehicles fuelled by hydrogen, either directly or through hydrogen fuel cells, may serve as examples of how close is the hydrogen age. Renewable hydrogen production is not popular yet because the cost is still high. Photovoltaic water electrolysis may become more competitive as the cost continues to decrease with the technology advancement; however, the considerable use of small band gap semiconducting materials may cause serious life cycle environmental impacts. Since hydrogen is recognized as an environmental friendly and a highly efficient fuel, the production of H₂ by direct water splitting attainable without polluted by-products is one of the potential alternatives to produce fuel for future energy supply. The utilization of an oxide semiconductor photocatalyst for water splitting is a promising technique because the photocatalyst is in the solid phase, which is relatively inexpensive, safe for operation, and resistant to deactivation and environmentally friendly production of hydrogen by solar energy. The diagram in Figure 2.1 shows that, while the introduction of fuel cell technology will lead to a substantial reduction in the emissions of greenhouse gases (expressed in carbon units per kilometer), the use of

fuel cells powered by hydrogen obtained from solar energy will reduce the emissions to nearly zero.

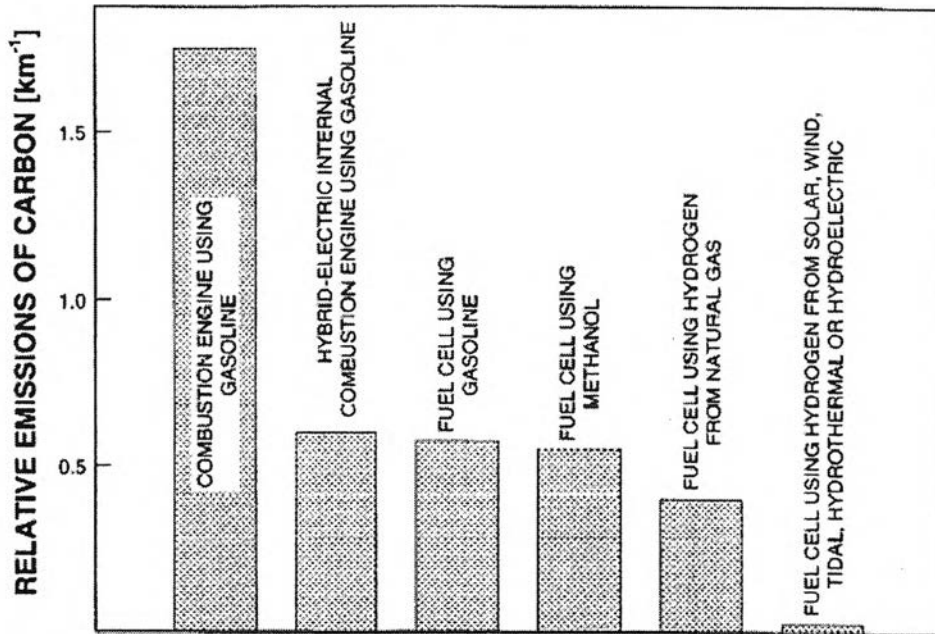


Figure 2.1 Relative emissions of greenhouse gases (expressed in carbon units per km) for vehicles powered by today’s internal combustion engine using gasoline compared to vehicles powered by fuel cells (Bak *et al.*, 2002).

2.2 Photocatalytic Water Splitting

2.2.1 Photocatalytic Reactions

Photocatalytic reactions have been extensively studied. Photocatalytic reactions are classified into two categories: “down-hill” and “up-hill” reactions. Degradation, such as photo-oxidation of organic compounds using oxygen molecules, is generally a down-hill reaction, of which the reaction proceeds irreversibly. In this reaction, a photocatalyst works as a trigger to produce O_2^- , HO_2 , OH^\bullet , and H^+ as active species for oxidation at the initial stage. This type of reaction is regarded as a photo-induced reaction, as depicted in Figure 2.2(a), and has been extensively studied using titanium dioxide photocatalyst (Fujishima *et al.*, 2000). On the other hand, water splitting reaction is accompanied by a largely positive change in the Gibbs free energy ($\Delta G^0 = 237 \text{ kJ/mol}$) and is an up-hill reaction. In this reaction, photon energy is converted into chemical energy, as also

shown in Figure 2.2(b), similar to photosynthesis by green plants. Therefore, this type of reaction is called artificial photosynthesis.

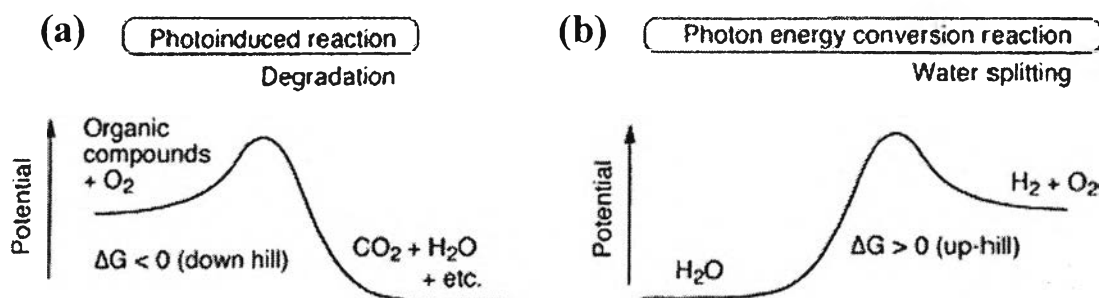


Figure 2.2 Types of photocatalytic reactions: (a) photoinduced reaction and (b) photon energy conversion reaction.

Since the first energy crisis in the early 1970s, much research has been devoted to the development of efficient systems that would enable the absorption and conversion of solar light into useful chemical energy resources. One of the most promising of such “artificial photosynthesis” a reaction is the photocatalytic splitting of water to produce H_2 and O_2 under solar light:



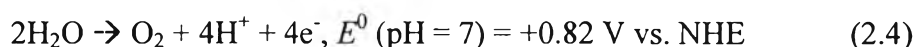
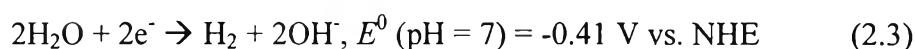
The refinement of this up-hill reaction is greatly desired not only for the conversion and storage of solar energy but also for the clean and safe production of hydrogen since the consumption of hydrogen will be expected to increase dramatically, especially for use in fuel cells.

2.2.2 Splitting Water into Hydrogen

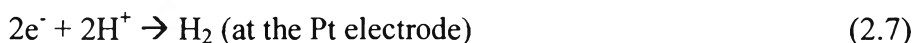
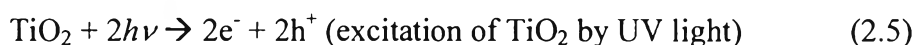
The technologies for hydrogen generation using sources of renewable energy are in the incubation stage. Photocatalytic splitting water into hydrogen has attracted extensive attention due to its potential to obtain clean and highly efficient hydrogen energy from abundant water. For about 35 years, since the work of Fujishima and Honda which reported on the photodecomposition of water over

semiconductor photoelectrolysis cells (Fujishima *et al.*, 1972), many studies in the photocatalytic splitting of water have been carried out. The energy conversion efficiency of water photoelectrolysis is primarily determined by the properties of materials used for the photoelectrodes.

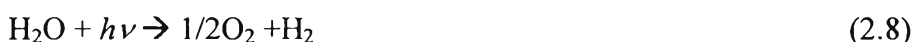
For photoelectrolysis of water, a potential difference of more than 1.23 eV is necessary between cathodic and anodic electrodes (Eq. (2.2)), where the following anodic and cathodic reactions take place simultaneously (Eq. (2.3) and (2.4)).



This potential difference is equivalent to the energy of a wavelength of approximately 1008 nm. Therefore, if the energy of light is used effectively in an electrochemical system, it should be possible to decompose water with visible light of wavelength shorter than 1008 nm. However, water is transparent to visible light, it cannot be decomposed by visible light alone. It can be split by irradiation alone only with ultraviolet light shorter than 190 nm. Fujishima and Honda were the first to study photodecomposition of water over semiconductor photoelectrolysis cells using light of wavelength $\lambda < 400$ nm. Photoelectrolysis cells consisting of a TiO₂ electrode and Pt black electrode are connected through an external load, as shown in Figure 2.3. Photo-irradiation of the TiO₂ electrode under a small electric bias led to the evolution of H₂ and O₂ at the surface of the Pt electrode and TiO₂ electrode, respectively.



The overall reaction can be expressed as Eq. (2.8):



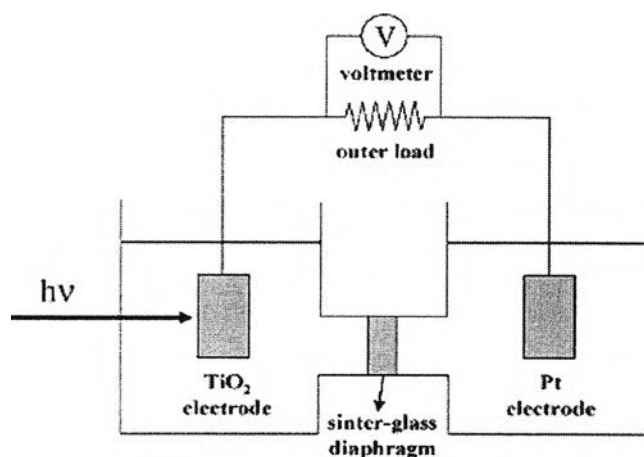


Figure 2.3 Electrochemical cell in which the TiO₂ electrode is connected with a Pt electrode (Matsuoka *et al.*, 2007).

Despite the success of Fujishima-Honda, use of a photoelectrochemical cells involves the difficulty of constructing the oxide semiconductor photoelectrode. Therefore, applications of the principle of water photodecomposition using semiconductor to heterogeneous photocatalytic systems using powdered semiconductors instead of photoelectrodes have been actively studied by reason of their advantages over photoelectrochemical cells, i.e. low cost to construct, chemical stability under the light, and large surface area. Such attempts have been supported by two experimental advances. One is accumulation of data on photocatalytic reactions over powdered semiconductors, while the other is Bard's concept that can be pictured as a "short-circuited" photoelectrochemical cell where semiconductor electrode and metal counter electrode have been brought into contact in single particle. The history and development of the briefly mentioned progress about water splitting can be traced as follows (Bard *et al.*, 1995).

2.2.3 Efficiency

The free energy change for water splitting reaction is $\Delta G^\circ = 237.2$ kJ/mol or 2.46 eV/molecule of H₂O. Since two electrons are involved in the reaction, this corresponds to 1.23 eV/e, which is also the standard emf for the reaction. The photons in the solar spectrum provide sufficient energy to drive this reaction, but the efficiency of the reaction depends upon how the reaction is carried out. It is possible

to cause water splitting thermally with light via concentrators and a solar furnace by heating water to 1,500-2,500 K. However, the efficiency of this process is typically below 2%, and the cost of the capital equipment and material stability problems suggest that this approach for water splitting is not a promising one.

Since water itself does not absorb appreciable radiation within the solar spectrum, one or more light-absorbing species, i.e. semiconductors as the photoconverters, must be used to transform the radiant energy to chemical (or electrical) energy in the form of electron/hole pairs, i.e. to the oxidizing and reducing potentials needed to drive the reaction. The maximum efficiency for photochemical water splitting has been considered in a number of papers and depends upon the band gap (or threshold energy), E_g , of the semiconductor. Radiation of energy below E_g is not absorbed while that above E_g is partly lost as heat by internal conversion or intraband thermalization processes. Additional thermodynamic losses occur because the excited state concentration is only a fraction of that of the ground state and because some excited states are lost through radiative decay (Archer *et al.*, 1990).

2.2.4 Semiconductor Photocatalyst

A semiconductor is a material with an electrical conductivity that is intermediate between that of an insulator and a conductor. Like other solids, semiconductor materials have electronic band structure determined by the crystal properties of the material. The actual energy distribution among electrons is described by the Fermi level and temperature of the electrons. Among the bands filled with electrons, the one with the highest potential level is referred to as the valence band (VB), while the band outside of this is referred to as the conduction band (CB). The energy width of the forbidden band between the valence band and the conduction band is referred to as the band gap (E_g). The overall structure of band gap energy is shown in Figure 2.4. The band gap can be considered as a wall that electrons must jump over in order to become free. When light is illuminated at appropriate wavelengths with energy equal or more than band gap energy, valence band (VB) electrons can move up to the conduction band (CB). At the same time, as

many positive holes as the number of electrons that have jumped to the conduction band (CB) are created.

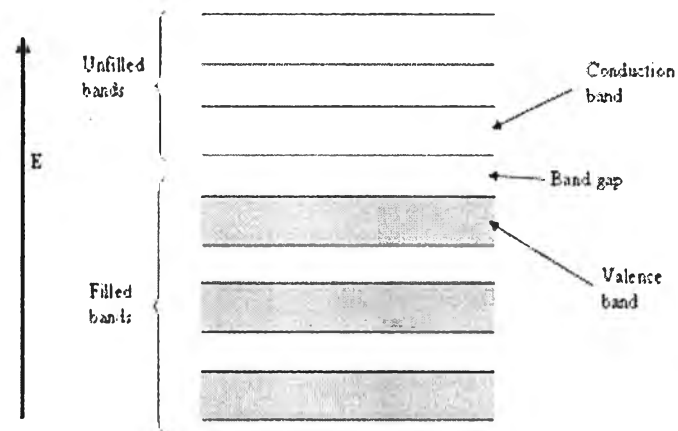


Figure 2.4 The structure of band gap energy.

2.2.5 Types of semiconductor systems proposed for solar water splitting

2.2.5.1 *Semiconductor Solid State Photovoltaic Based Systems*

A number of different approaches are possible with semiconductors. The most direct approach employs a solid state photovoltaic solar cell to generate electricity that is then passed into a commercial-type water electrolyzer, as shown in Figure 2.5(a). The electrolysis of water at a reasonable rate in a practical cell requires applied voltages significantly larger than the theoretical value (1.23 V at 25°C). Moreover, the components are rugged and should be long-lived. The problem with such a system is its cost. Solar photovoltaics cannot currently produce electricity at competitive prices, and hydrogen from water electrolyzers is significantly more expensive than that produced chemically from coal or natural gas.

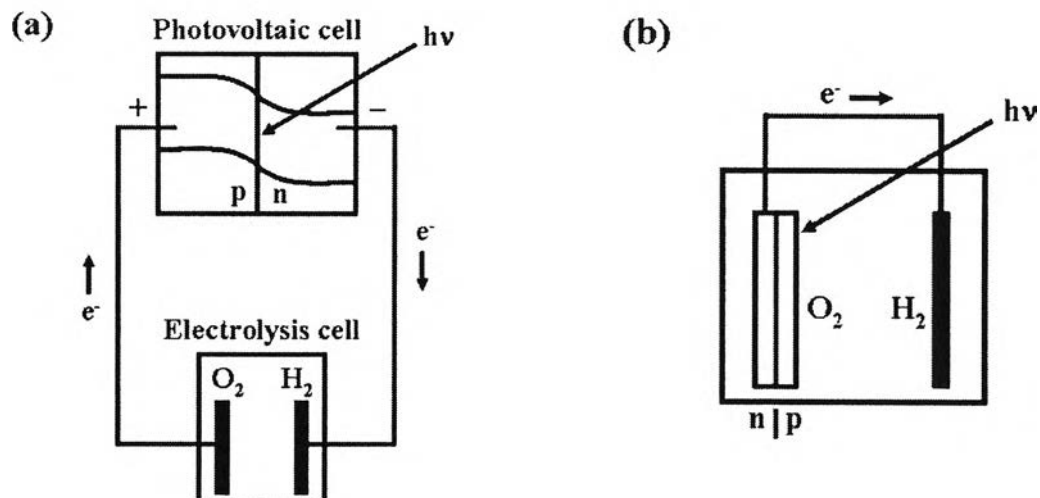


Figure 2.5 Schematic of (a) solid state photovoltaic cell driving a water electrolyzer and (b) cell with immersed semiconductor p/n junction (or metal/semiconductor Schottky junction) as one electrode.

An alternative system involves the semiconductor photovoltaic cell immersed directly in aqueous system, as illustrated in Figure 2.5(b). At the least, this eliminates the costs and mechanical difficulties associated with separate construction and interconnection of solar and electrochemical cells. In one such system, the electrodes are composed of single or multiple semiconductor p/n junctions that are irradiated while they are within the cell. This simpler apparatus is attained at the cost of encapsulating and coating the semiconductors to protect them from the liquid environment and probably with a more limited choice of electrocatalyst for H_2 or O_2 evolution. Note that, in addition to p/n semiconductor junctions, those between a metal and semiconductor (Schottky barriers) can also be used to produce a photopotential.

2.2.5.2 Semiconductor Electrode (Liquid Junction) Systems

Of more interest are systems, in which the photopotential to drive the water splitting reaction is generated directly at the semiconductor/liquid interface, as shown in Figure 2.6. Rather extensive research was carried out on various metal electrodes, sometimes covered with oxide or other films, and immersed in a variety of solutions, including some containing fluorescent dyes. The discovery

of the transistor and interest in semiconductor materials led to more extensive electrochemical and photoelectrochemical studies, usually with the goal of characterizing the semiconductor.

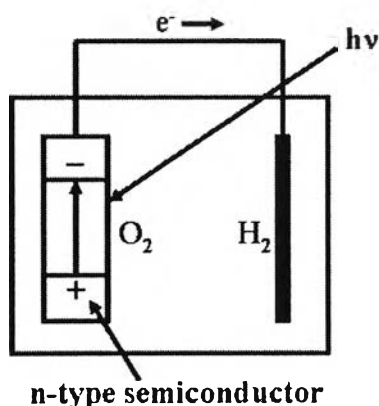


Figure 2.6 Schematic of liquid junction semiconductor electrode cell.

The modern era of semiconductor electrodes and interest in these in photoelectrochemical devices for energy conversion, especially via the water splitting reaction, can be cited to the work of Fujishima and Honda on single-crystal TiO_2 electrodes (Fujishima *et al.*, 1972). Indeed, water splitting in TiO_2 -based cells can be accomplished, but only with an additional electrical bias. The problem with TiO_2 is that the conduction band is too low, i.e. at an insufficiently negative potential, to generate hydrogen at a useful rate. Moreover, because the TiO_2 band gap is too large (3.2 eV for anatase and 3.0 eV for rutile), only a small fraction of the solar light is absorbed. Cells with TiO_2 electrodes of various types, e.g. single crystal, polycrystal, and thin film, have nevertheless been heavily investigated, largely because TiO_2 is very stable and is a good model for understanding the semiconductor/liquid interface.

2.2.5.3 Semiconductor Particle Systems

A considerable simplification of the apparatus is possible if the electrochemical cell can be replaced by simple dispersions of semiconductor particles. In such dispersions, the semiconductor particles can be coated with islands of metals or metal oxides that behave as catalytic sites, with each particle behaving as a microelectrochemical cell, as shown in Figure 2.7. TiO_2 has been a favorite material, although other compounds, such as CdS and ZnO, have also been studied.

While a number of interesting photoreactions have been carried out, including the use of particles to destroy organics and to plate metals from waste water (Ollis *et al.*, 1993) and for synthetic purposes (Serpone *et al.*, 1989), reports on the use of particulate systems for water splitting remain controversial. An extension of this approach is the use of colloidal-sized particles down to nanoparticles. Such small particles also have very high surface areas that, in principle, allow faster capture of the photogenerated charges by solution species and with less bulk recombination.

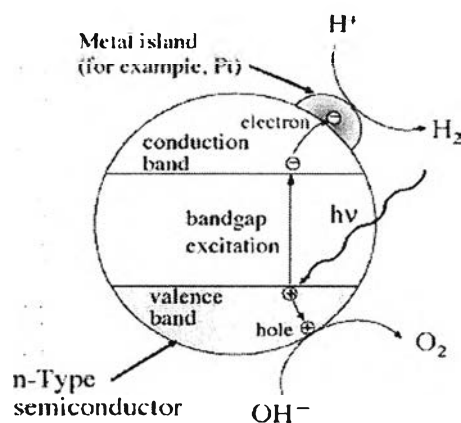


Figure 2.7 Representation of semiconductor particulate systems for heterogeneous Photocatalysis (Matsuoka *et al.*, 2007).

2.2.6 The Principle of Water Splitting Using Semiconductor Particle

The principle of water splitting using a semiconductor photocatalyst is shown in Figure 2.8. The semiconductor photocatalyst absorbs impinging photons with energies equal to or higher than its band gap or threshold energy. Each photon of the required energy (i.e. wavelength) that strikes an electron in the occupied valence band (VB) of the semiconductor atom can elevate that electron to the unoccupied conduction band (CB), leading to excited state conduction band electrons and positive valence band holes (Serpone *et al.*, 1989). The photogenerated electrons and holes cause redox reactions similar to electrolysis. Water molecules are reduced by the electrons to form H₂ and oxidized by the holes to form O₂, leading to overall water splitting. The width of the band gap and the potentials of the conduction and valence bands are important for the semiconductor photocatalyst material. The bottom level of the conduction band (CB) has to be more negative than the reduction potential of H⁺/H₂ (0 V vs NHE), while the top level of

the valence band (VB) has to be more positive than the oxidation potential of O_2/H_2O (1.23 V).

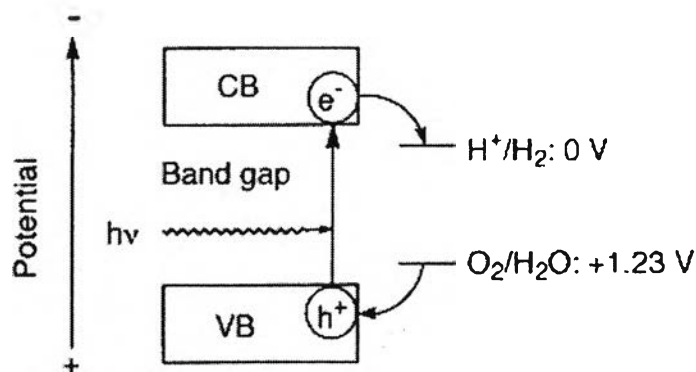


Figure 2.8 Reaction schematic for water splitting reaction over semiconductor photocatalysts.

The competition between charge carrier recombination and charge carrier trapping followed by the competition between recombination of trapped carriers and interfacial charge transfer are what determine the overall quantum efficiency for interfacial charge transfer. Also of great importance are the band positions or flat band potentials of the semiconductor material. These indicate the thermodynamic limitations for the photoreactions that can take place.

However, the potential of the band structure is just the thermodynamic requirement. Other factors, such as charge separation, mobility, and lifetime of photogenerated electrons and holes, also affect the photocatalytic properties, as shown in Figure 2.9, in which the fate of these charge carriers may take different paths. Firstly, they can get trapped in the bulk either in shallow or in deep traps. Secondly, they can recombine, non-radiatively or radiatively, dissipating the input energy as heat. Finally, they can react with electron donors or acceptors adsorbed on the surface of the photocatalyst (Hoffmann *et al.*, 1995). These properties are strongly influenced by bulk properties of the material, such as crystallinity. Surface properties, such as surface area and active reaction sites, are also imperative. Cocatalysts, such as Pt and NiO, are often loaded on the surface in order to introduce active sites for H_2 evolution. Thus, suitable bulk and surface properties and energy structure are demanded for photocatalysts. So, one can state that the photocatalyst is a highly functional material.

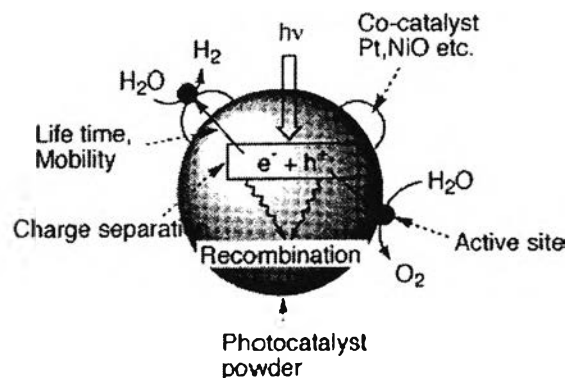


Figure 2.9 Processes occurring in semiconductor photocatalyst under photoexcitation for water splitting reaction.

2.3 Photocatalysts

Since water is transparent to solar radiation, direct decomposition of water by solar light is not viable. Energetically, it seems relatively easy to photocatalyze water, since the theoretical minimum photovoltage required for this process is only 1.23 eV. Semiconductors, in the presence of light energy, are capable of decomposing water into hydrogen and oxygen depending upon energy levels of their conduction and valence bands. In an ideal system, conduction band level should be well above (more negative than) the water reduction level, and valence band edge should be well below (more positive than) the water oxidation level for an efficient production of hydrogen and oxygen from water by photolysis, as shown in Figure 2.10. Some of the photocatalysts that satisfy both conditions are SrTiO_3 , CaTiO_3 , TiO_2 , $\text{Sr}_2\text{Nb}_2\text{O}_5$, $\text{Sr}_2\text{Ta}_2\text{O}_7$, ZnO , CdS , NiO , etc.

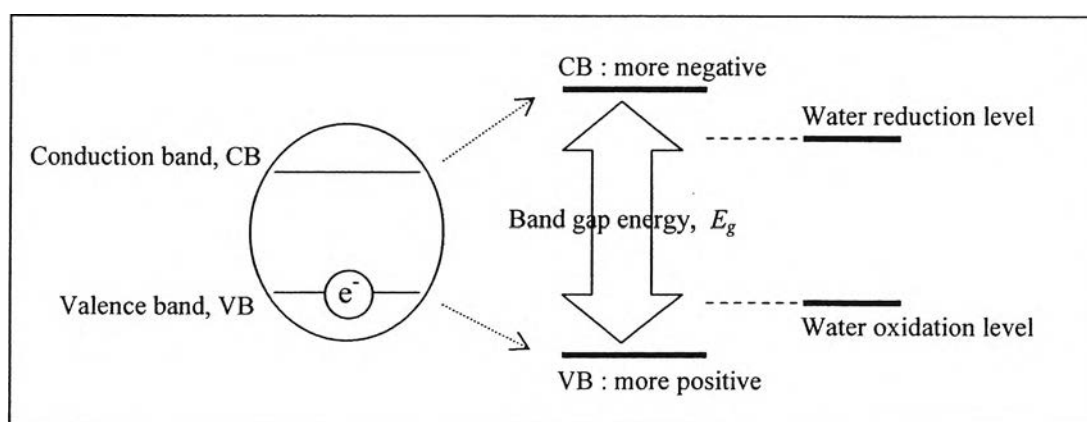


Figure 2.10 Band gap energy of the photocatalyst.

Powders with semiconductor characteristics have been widely employed in photocatalytic systems because they are capable of generating charge carriers by absorbing photon energies. The separation effectiveness of the photo-induced charge carriers is an important factor in determining the photocatalytic activity of the powders. One promising photocatalyst is perovskite-related material. Perovskite-related materials are represented by the general formula of ABO_3 (A = rare earth and alkali element with or without its partial substitution by alkaline earth element, and B = transition element, such as Co, Mn, Ti, Ta, Ni, Fe, etc., with or without its partial substitution). The interest of these materials for the photochemical splitting of water derives from the possibility to use their interlayer space for reaction sites, where electron-hole recombination process could be retarded by physical separation of electron and hole pairs generated by photo-absorption. Perovskite-like $NaTaO_3$ loaded with NiO cocatalyst exhibited high activity in water splitting under UV light irradiation. The NiO cocatalyst promotes the transfer of photo-induced electrons in the conduction band of $NaTaO_3$ and enhances charge separation. The sol-gel-synthesized $NaTaO_3$ possessed the monoclinic phase, which was found to have a larger number of effective states available for the photo-induced electrons and holes. As to crystalline structure, the bond angle of Ta–O–Ta for the monoclinic phase was close to 180° , a value ideal for delocalization of the excited energy in tantalate crystals (Hu *et al.*, 2007).

Calcium titanate ($CaTiO_3$) belongs to the family of the perovskite ABO_3 structure. Platinized $CaTiO_3$ powder had a high photocatalytic activity of decomposing water into H_2 and O_2 under the irradiation of UV light. The band gap energy (E_g) of $CaTiO_3$ is about 3.5 eV, being capable of generating conductive carriers in this system. The value of the energy is also consistent with the E_g estimated based on reflectance spectra recorded from $CaTiO_3$ single crystal, with value of -0.78 V versus saturated calomel electrode (SCE). This implies that the position of the conduction band for $CaTiO_3$ is slightly higher than the ionization potential of H_2 (0 V), and therefore this material has a potential for decomposing water (Mizoguchi *et al.*, 2002).

Strontium titanate ($SrTiO_3$) is a well-known cubic-perovskite paraelectric oxide with a large dielectric constant, which has attracted a great deal of attention

due to its excellent dielectric, photoelectric, optical, and catalytic properties. SrTiO₃ is also considered to be useful for photocatalytic decomposition of water in place of conventional photocatalysts, such as TiO₂, because its CB level provides a higher photopotential than TiO₂ and facilitates hydrogen and oxygen formation (Subramanian *et al.*, 2006). However, pure SrTiO₃ without cocatalysts showed very low photocatalytic activity. Therefore, the modification of SrTiO₃ is necessary to obtain active catalysts for H₂ and O₂ generation from pure water. For example, Ag, Cr, Pt, Rh, Pd, and Ta have been incorporated into SrTiO₃. The photocatalytic activity enhancement by Ag doping on SrTiO₃ was reported by Subramanian *et al.* (2006). SrTiO₃ doped with Cr³⁺ led to an introduction of isolated energy levels within its band gap, so photon can be absorbed at two levels, the band gap and the sub-band gap, where the latter led to light absorption in the visible region (Ashokkumar, 1998).

Zielińska *et al.* (2008) have investigated the photocatalytic efficiency of alkaline earth titanate-based compounds (Ca, Sr, Ba) for hydrogen generation. Their results showed that the addition of organic donors (such as formic acid, acetic acid, methanol, 2-propanol, and formaldehyde) enhanced the efficiency of the studied process. The systematic study has shown that the most efficient organic donor in regards to its hydrogen generation efficiency was formic acid. Of the catalysts explored, the highest photocatalytic activity was obtained by using SrTiO₃:TiO₂ composite.

2.4 Nano-Photocatalysts

2.4.1 General Remarks

Nanocrystalline photocatalysts are ultras-small semiconductor particles, which are few nanometers in size. During the past decade, the photochemistry of nanosized semiconductor particles has been one of the fastest growing research areas in physical chemistry. The interest in these small semiconductor particles originates from their unique photophysical and photocatalytic properties. Several review articles have been published concerning the photophysical properties of nanocrystalline semiconductors. Such studies have

demonstrated that some properties of nanocrystalline semiconductor particles are in fact different from those of bulk materials.

Nanosized particles possess properties which fall into the region of transition between the molecular and bulk phases. In the bulk material, the electron excited by light absorption finds a high density of states in the conduction band, where it can exist with different kinetic energies. In the case of nanoparticles, however the particle size is the same as or smaller than the size of the first excited state. Thus, the electrons and holes generated upon illumination cannot suit into such a particle, unless they assume a state of higher kinetic energy. Hence, as the size of the semiconductor particle is reduced below a critical diameter, the spatial confinement of the charge carriers within a potential well, like “a particle in a box”, causes them to mechanically behave quantum. In solid state terminology, this means that the bands split into discrete electronic states (quantized levels) in the valence and conduction bands, and the nanoparticle progressively behaves similar to a giant atom. Nanosized semiconductor particles, which exhibit size-dependent optical and electronic properties, are called quantized particles or quantum dots (Kamat., 1995).

2.4.2 Activity of Nano-Photocatalysts

One of the main advantages of the application of nanosized particles is the increase in the band gap energy with decreasing particle size. As the size of a semiconductor particle falls below the critical radius, the charge carriers begin to behave mechanically quantum, and the charge confinement leads to a series of discrete electronic states. As a result, there is an increase in the effective band gap and a shift of the band edges. Thus by varying the size of the semiconductor particles, it is possible to enhance the redox potential of the valence band holes and the conduction band electrons.

However, the solvent reorganizational free energy for charge transfer to a substrate remains unchanged. The increasing driving force and the unchanged solvent reorganizational free energy are expected to lead to an increase in the rate constants for charge transfer at the surface. The use of nanosized semiconductor particles may result in increased photocatalytic activity for systems, in which the rate-limiting step is interfacial charge transfer. Hence, nanosized semiconductor

particles can possess enhanced photoredox chemistry with reduction reactions, which might not otherwise proceed in bulk materials, being able to occur readily using sufficiently small particles. Another factor, which could be advantageous, is the fact that the fraction of atoms that are located at the surface of a nanoparticle is very large. Nanosized particles also have high surface area to volume ratios, which further enhances their catalytic activity. One disadvantage of nanosized particles is the need for light with a shorter wavelength for photocatalyst activation. Thus, a smaller percentage of a polychromatic light source will be useful for photocatalysis.

In large TiO₂ particles (Zhang *et al.*, 1998), volume recombination of the charge carriers is the dominant process and can be reduced by a decrease in particle size. This decrease also leads to an increase in the surface area, which can be translated as an increase in the available surface active sites. Thus, a decrease in particle size should also result in higher photonic efficiencies due to an increase in the interfacial charge carrier transfer rates. However, as the particle size is lowered below a certain limit, surface recombination processes become dominant, since firstly most of the electrons and holes are generated close to the surface, and secondly surface recombination is faster than interfacial charge carrier transfer processes. This is the reason why there exists an optimum particle size for maximum photocatalytic efficiency.

2.5 Chemical Additive for Enhancement of Photocatalytic H₂ Production

Due to rapid recombination of photogenerated CB electrons and VB holes, it is difficult to achieve water splitting for hydrogen production using TiO₂ photocatalyst in pure distilled water. Adding electron donors (sacrificial reagents or hole scavengers) to react irreversibly with the photogenerated VB holes can enhance the photocatalytic electron/hole separation, resulting in higher quantum efficiency. Since electron donors are consumed in photocatalytic reaction, continual adding of electron donors is required to sustain hydrogen production.

Organic compounds (hydrocarbons) are widely used as electron donors for photocatalytic hydrogen production as they can be oxidized by VB holes. The remaining strong reducing CB electrons can reduce protons to hydrogen

molecules. EDTA, methanol, ethanol, CN⁻, lactic acid, and formaldehyde have been tested and proved to be effective to enhance hydrogen production. Nada *et al.* (2005) carried out a qualitative investigation to study the effects of different electron donors on hydrogen production. The rankings in terms of the degree of hydrogen production enhancement capability were found to be: EDTA > methanol > ethanol > lactic acid. It should be noted that the decomposition of these hydrocarbons could also contribute to a higher hydrogen yield since hydrogen is one of their decomposed products. Other inorganic ions, such as S²⁻/SO₃²⁻, Ce⁴⁺/Ce³⁺, and IO₃⁻/I⁻ were also used as sacrificial reagents for hydrogen production. When CdS is used as photocatalyst for water splitting hydrogen production, photocorrosion occurs as follows:



By serving as a sacrificial reagent, S²⁻ can react with 2 holes to form S. The aqueous SO₃²⁻ added can dissolve S into S₂O₃²⁻ in order to prevent any detrimental deposition of S onto CdS. Therefore, photocorrosion of CdS is prevented. In another system of using inorganic ions, I⁻ (electron donor) and IO₃⁻ (electron acceptor) work as a pair of redox mediators. Two photocatalysts were employed to produce H₂ and O₂ under the mediation of I⁻ and IO₃⁻, respectively. For hydrogen production on the photocatalyst with more negative CB level, I⁻ can scavenge holes and, thus, CB electrons are available to reduce protons to hydrogen molecules. For oxygen production on the photocatalyst with more positive VB level, IO₃⁻ can react with CB electrons to form I⁻ and, thus, VB holes can oxidize water to oxygen. In this system, photocatalytic water splitting produces both hydrogen and oxygen without consumption of the sacrificial reagent, as illustrated in Figure 2.11. As rutile has unique selectivity in oxidation, oxygen molecules are evolved. For comparison, IO₃⁻ anions are produced on the surface of anatase. Therefore, the combination of anatase and rutile shows a higher hydrogen production rate under the mediation of I⁻/IO₃⁻ pairs. Similarly, Ce⁴⁺/Ce³⁺ and Fe³⁺/Fe²⁺ pairs are also effective for water splitting hydrogen production.

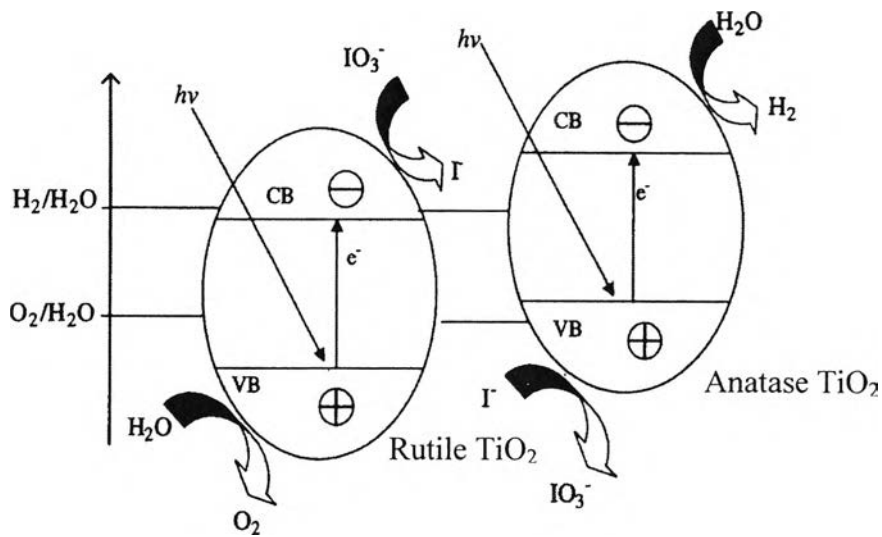


Figure 2.11 Photocatalytic hydrogen production over anatase/rutile TiO_2 under the mediation of I^-/IO_3^- .

2.6 Photocatalyst Modification Techniques for Enhancement of H_2 Production

2.6.1 Noble Metal Loading

Noble metals, including Pt, Au, Pd, Rh, Ni, Cu, and Ag, have been reported to be very effective for enhancement of TiO_2 photocatalysis. As the Fermi levels of these noble metals are lower than that of TiO_2 , photoexcited electrons can be transferred from conduction band to metal particles deposited on the surface of TiO_2 , while photogenerated valence band holes remain on the TiO_2 . These activities greatly reduce the possibility of electron-hole recombination, resulting in efficient separation and stronger photocatalytic reactions. As electrons accumulate on the noble metal particles, their Fermi levels shift closer to the conduction band of TiO_2 , resulting in more negative energy levels. This is beneficial for water splitting for hydrogen production. Furthermore, smaller metal particles deposited on TiO_2 surface exhibit more negative Fermi level shift. Accumulated electrons on metal particles can then be transferred to protons adsorbed on the surface and further reduce the protons to hydrogen molecules. Therefore, noble metals with suitable work function can help electron transfer, leading to higher photocatalytic activity. Bamwenda *et al.* (1995) compared hydrogen production from water-ethanol solution using Au-loaded TiO_2 and Pt-loaded TiO_2 as photocatalysts. It was found that loading of Pt worked better than loading of Au. Sakthivel *et al.* (2004) investigated photooxidation of Acid

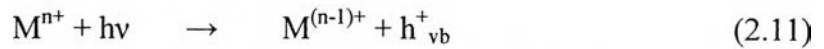
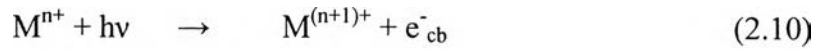
Green 16 using Pt, Au, and Pd-loaded TiO₂ as photocatalysts. Optimal loading was observed in their experiments. Too much metal particle deposition might reduce photon absorption by TiO₂ and might also become electron-hole recombination centers, resulting in lower efficiency. Loadings of Pt and Au were more effective than loading of Pd because of suitable electron affinity and work function of Pt and Au. It should be noted that although the loading of noble metal can reduce recombination to some extent, hydrogen production from pure water splitting is difficult to achieve, because: (i) recombination cannot be completely eliminated; and (ii) backward reaction of H₂ and O₂ to form H₂O is thermodynamically favorable. Therefore, as discussed in the previous sections, electron donors or carbonate salts, as well as other mediators, are required to avoid the above listed problems. Since Pt is very expensive, more research is needed to identify low-cost metals with acceptable enhancement of photocatalytic activity. For example, Dhanalakshimi *et al.* (2000) investigated dye-sensitized hydrogen production. When Pt/TiO₂ and Cu/TiO₂ were used as photocatalysts, enhanced hydrogen production was observed, and the effect of Cu loading was almost comparable to Pt loading. Unlike dye sensitization, Wu and Lee (2004) deposited Cu particles on TiO₂ surface for hydrogen production from methanol solution. At the optimal loading of Cu, hydrogen production rate was enhanced as much as 10 times higher. Other low-cost metals, such as Ni and Ag, were also found to be effective for photocatalytic activity enhancement. These low-cost but effective metals are expected to be promising materials to improve photocatalytic activities of TiO₂ for practical applications. For photocatalytic hydrogen production, Pt is mostly considered by several researchers to be the most effective cocatalyst and is widely used, resulting in considerably high H₂ evolution efficiency.

2.6.2 Ion Doping

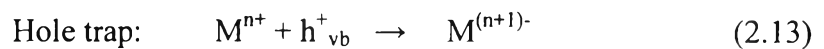
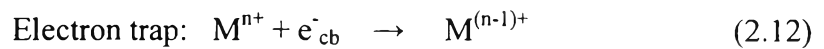
2.6.2.1 *Metal Ion Doping*

Transitional metal ion doping and rare earth metal ion doping have been extensively investigated for enhancing the TiO₂ photocatalytic activities. Choi *et al.* (1994) carried out a systematic investigation to study the photoreactivity

of 21 metal ions doped into TiO₂. It was found that doping of metal ions could expand the photo-response of TiO₂ into visible spectrum. As metal ions are incorporated into the TiO₂ lattice, impurity energy levels in the band gap of TiO₂ are formed, as indicated below:



where M and Mⁿ⁺ represent metal and the metal ion dopant, respectively. Furthermore, electron and hole transfer between metal ions and TiO₂ can alter electron/hole recombination as:



The energy level of Mⁿ⁺/M⁽ⁿ⁻¹⁾⁺ should be less negative than that of the conduction (CB) edge of TiO₂, while the energy level of Mⁿ⁺/M⁽ⁿ⁺¹⁾⁺ should be less positive than that of the valance band (VB) edge of TiO₂. For photocatalytic reactions, carrier transferring is as important as carrier trapping. Only if the trapped electron and hole are transferred to the surface, photocatalytic reactions can occur. Therefore, metal ions should be doped near the surface of TiO₂ particles for a better charge transferring. In case of deep doping, metal ions likely behave as recombination centers, since electron/hole transferring to the interface is more difficult. Furthermore, there exists an optimum concentration of doped metal ion, above which the photocatalytic activity decreases due to the increase in recombination. Among the 21 metal ions studied, Fe, Mo, Ru, Os, Re, V, and Rh ions can increase photocatalytic activity, while dopants Co and Al ions cause detrimental effects. The different effects of metal ions result from their abilities to trap and transfer electrons/holes. For example, Cu and Fe ions can trap not only electrons but also holes, and the impurity energy levels introduced are near to conduction band, as well as valance band edges of TiO₂. Therefore, doping of either Cu or Fe ions could be recommended for enhancement of photocatalytic activity.

Peng *et al.* (2004) investigated the effect of Be ion-doped TiO₂ on photocatalytic hydrogen production in the presence of electron donor (ethanol). It was found that doping the metal ions near the surface was beneficial for

charge carrier transferring, while deep doping led to poor performance. Furthermore, doping content and preparation methods could also affect photocatalytic hydrogen production. Under optimal condition of Be ion doping into TiO₂, hydrogen production was found to be 75% higher than that of un-doped TiO₂. Extensive research on metal ion doping method for enhancement of TiO₂ photocatalytic activities has been carried out, especially for water/air cleaning applications. Organic compounds adsorbed by the photocatalysts are decomposed mainly by the valence band holes and radicals induced by holes. Therefore, the mechanism involved in transferring these photogenerated holes to the interface is of paramount importance. On the other hand, for photocatalytic hydrogen production, the transfer of conduction band electrons to the interface and their energy levels are the most important factors that affect the hydrogen production rate. Hence, the results based on water/air cleaning applications cannot be directly applied to hydrogen production. Besides, the TiO₂ photocatalytic effect is very sensitive to the metal ion doping methods, doping content, and doping depth. Therefore, a systematically comparative investigation is needed in order to characterize photocatalytic hydrogen production enhanced by metal ion doping.

2.6.2.2 Anion Doping

The use of anion doping to improve hydrogen production under visible light is rather a new method with few investigations reported in open literature. Doping of anions (N, F, C, S etc.) in TiO₂ crystalline could shift its photo-response into visible spectrum. Unlike metal ions (cations), anions less likely form recombination centers and, therefore, are more effective to enhance the photocatalytic activity. Asahi *et al.* (2001) determined the substitutional doping contents of C, N, F, P, and S for O in anatase TiO₂. It was found that mixing of p states of N with 2p of O could shift VB edge upwards to narrow down the band gap of TiO₂. Although doping of S had resulted in a similar band gap narrowing, the ionic radius of S was reported to be too large to be incorporated into the lattice of TiO₂. Dopants C and P were found to be less effective as the introduced states were so deep that photogenerated charge carriers were difficult to be transferred to the surface of the catalyst.

The nitrogen doped TiO₂ thin film was prepared by sputtering TiO₂ in an N₂ (40%)/Ar gas mixture, followed by annealing at 550°C in N₂ for about 4 h. Nitrogen doped TiO₂ powder was also prepared by treating TiO₂ in NH₃ (67%)/Ar at 600°C for 3 h. The N-doped TiO₂ was reported to be effective for methylene blue decomposition under visible light ($\lambda > 400$ nm). Additionally, it was reported by Umebayashi *et al.* (2002) that S-doped TiO₂ could be prepared by oxidation annealing of TiS₂. Annealed at 600°C, TiS₂ was partly changed to anatase TiO₂. The residual S atoms in the anatase TiO₂ formed S-doped TiO₂ by Ti–S bonds. Band structures of the S-doped TiO₂ were calculated using the super cell approach. It was found that when TiO₂ was doped with S, the mixing of S3p states with the valence band of TiO₂ increased the width of valence band, resulting in band gap narrowing. Since the band gap narrowing was caused by valence band upward shifting, the conduction band remained unchanged. Therefore, the S-doped TiO₂ should be able to reduce protons for hydrogen production under visible light. On the other hand, the upward shift of valence band may reduce the oxidation ability under visible light. Ohno *et al.* (2004) developed a new method to prepare S-doped TiO₂ powder. Titanium isopropoxide was mixed with thiourea in ethanol and stirred. After subsequent evaporation, aging, and calcination, S-doped TiO₂ powder was obtained. The S ions were incorporated to replace some of the Ti atoms in the form of S⁴⁺. The photocatalytic activity of S-doped TiO₂ was then evaluated by photodecomposition of 2-propanol and methylene blue. It was reported that S-doped TiO₂ worked better than pure TiO₂ under visible light irradiation. Although the valence band was shifted upwards, the oxidation ability was found to be still high. Other anions, such as C and F ions, have also been investigated and found to be able to expand photo-response in visible spectrum.

Reddy *et al.* (2005) investigated the absorption of TiO₂, which is extended into the visible light region by doping with anion S, N, and C. The results showed that all anions could improve absorption of TiO₂ by reducing the band gap energy. The feature was more evident in N-doped TiO₂ compared to C and S, because N-doped TiO₂ showed two band gap transitions. The first one was in the UV region (385 nm), which is accounted for the fundamental band transition of TiO₂, and the second in the visible region (495 nm), as a result of nitrogen doping.

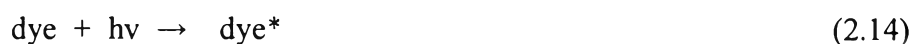
The distinction between two surface states was reflected as individualistic redox peaks. In contrast, the C- and S-doped samples did not show a sharp absorption edge as observed for pure TiO₂. This would imply that the doping introduces electronic states in the band gap that are spread across the band gap, resulting in a diffused absorption spectrum.

N-doped TiO₂ has been the most extensively investigated. The reported methods to dope N are heating of titanium hydroxide and urea, reactive DC magnetron sputtering, nitriding of anatase TiO₂ with alkylammonium salts, and treating TiO₂ powder in NH₃ (80%)/Ar gas flow at 550°C. Similar to S-doping, N-doping also caused a valence band upward shift, resulting in a narrow band gap and less oxidating holes. Mrowetz *et al.* (2004) reported that N-doped TiO₂ was unable to oxidize HCOO⁻. However, for hydrogen production, electrons are responsible for reducing protons, and the ability of oxidation does not affect the performance because the valence level of TiO₂ is far more positive than oxygen evolution energy level, and the conduction band remains almost unchanged after N-doping, being at a more negative than hydrogen production energy level. This throws a possibility that N-doped TiO₂ should be able to reduce protons for hydrogen production, although intensive researches have not been investigated. Under visible light irradiation, electrons can be promoted from energy levels in the band gap formed by nitrogen doping to conduction band. However, electron-hole recombination possibility of N-doped TiO₂ was reported to be higher than undoped TiO₂ (Torres *et al.*, 2004). For efficient photocatalytic reaction, coupling with other technologies, such as noble metal loading or electron donor addition, is necessary.

2.6.3 Dye Sensitization

Dye sensitization is widely used to utilize visible light for energy conversion. Some dyes having redox property and visible light sensitivity can be used in solar cells, as well as photocatalytic system (Gurunathan *et al.*, 1997). Under illumination by visible light, the excited dyes can inject electrons to CB of semiconductors to initiate the catalytic reactions, as illustrated in Figure 12. Even without semiconductors, some dyes, for example safranin O/EDTA and T/EDTA, are able to absorb visible light and produce electrons as reducing agents strong

enough to produce hydrogen (Bi and Tien, 1984). Nevertheless, without semiconductors acting as efficient charge separators, the rate of hydrogen production merely by dyes is very low. High hydrogen production rate can be obtained by efficient absorption of visible light and efficient transfer of electrons from excited dyes to CB of TiO₂. The CB electrons can then be transferred to noble metal particle (Pt) loaded on surface to initiate water reduction. In order to regenerate dyes, redox systems or sacrificial agents, such as I₃⁻/I⁻ pair and EDTA, can be added to the solution to sustain the reaction cycle. The excitation, electron injection, and dye regeneration can be expressed as follows:



To obtain a higher efficiency in converting absorbed light into direct electrical energy (for solar cells) or hydrogen energy, fast electron injection and slow backward reaction are required. Based on the literature on electron/hole recombination of dyes, the recombination times were found to be mostly in the order of nanoseconds to microseconds, sometimes in milliseconds, while the electron injection times were in the order of femtoseconds. The fast electron injection and slow backward reaction make dye-sensitized semiconductors feasible for energy conversion. Dhanalakshmi *et al.* (2000) carried out a parametric investigation to study the effect of using [Ru(dcpy)₂(dpq)]²⁺ as a dye sensitizer on photocatalytic hydrogen production from water under visible light irradiation. It was found that hydrogen production rate was enhanced by absorbing dye molecules to the TiO₂. The optimal combination of catalyst and Pt loading was found. Additional Pt or dye loading beyond the optimal values, hydrogen production rate did not further increase. This phenomenon indicated that only dye molecules adsorbed on the surface of TiO₂ could effectively inject electrons into TiO₂ for water reduction.

Gurunathan *et al.* (1997) investigated the effects of different dyes on photocatalytic hydrogen production by SnO₂ with and without a sacrificial agent, such as EDTA. The band gap of SnO₂ is 3.5 eV and, hence, it could not be excited by visible light. After SnO₂ was sensitized by dyes, hydrogen production was observed under visible light illumination. Qualitatively, the ranking of dyes in terms of the

degree of enhancement of hydrogen production rate was found in the following order: eosin blue > rose Bengal > Ru(bpy)₃²⁺ > rhodamine B ~ acriflavin > fluorescein. However, based on the structures and properties of these dyes, a general conclusion could not be drawn. For example, rhodamine B showed the longest absorption wavelength maxima together with more negative reduction potential (-0.545 V) than CB level (-0.34 V) of SnO₂, but it did not increase hydrogen production rate significantly. Therefore, the difference in their electron injection characteristics may be the reason for the variation in hydrogen production rates. However, comparison of electron injection characteristics among these dyes was not available. Further research work is thus required to compare dynamics of charge excitation, recombination, and electron injection of different dyes to gain a better understanding of the mechanisms behind the phenomena. Sensitization of TiO₂ particles platinized and suspended in water was carried out by Ru(bpy)₃²⁺, tris (bipiridine) Ru (II) (Ru(bpym)₃²⁺), and porphines to induce hydrogen evolution by visible light in the presence of sacrificial electron donor, EDTA. It found that Ru(bpym)₃²⁺ is an efficient sensitizer for hydrogen formation, which could be explained by the higher affinity of Ru(bpym)₃²⁺ on the TiO₂ surface than the Ru(bpy)₃²⁺ (Hirano *et al.*, 2000). In addition, high concentration of the Ru(bpy)₃²⁺ was required to achieve the photosensitization, suggesting adsorption of the sensitizer on the TiO₂. Sensitization of the TiO₂ particles for utilizing visible light has been an important subject both in photochemical energy conversion and decomposition of hazardous substances. In the sensitization of TiO₂ photoanode, adsorption of a dye to the semiconductor is an important condition to achieve the sensitization. The photoconversion efficiency was estimated from the amount of evolved hydrogen. Only under high concentration of sensitizer, the hydrogen formation took place efficiently with visible light. In these conditions, most of the incident photons are absorbed by sensitizer because of the competition between hydrogen evolution (second-order reaction) and the recombination of the separation charges (first-order reaction), and the difference of the photoinjection efficiency between the adsorbed dye and the free dye in the solution. In conventional hydrogen formation system by UV irradiation using platinized TiO₂ suspension and sacrificial donor in water, methanol is effective as a donor, leading to efficient hydrogen production, in which the methanol scavenges the

hold formed in the TiO_2 by direct excitation. In the present system, methanol does not work at all as a donor, supporting that the present system is a sensitized one, which does not produce holes in the TiO_2 bulk.

Recently, the new water splitting approach has been to combine two photocatalytic reactions, i.e. water reduction and water oxidation via some redox mediators, in order to divide the large energy required for the water splitting in two steps. Some workers had reported that the mixture of some xanthene dye and Pt- TiO_2 in aqueous triethanolamine solution exhibited hydrogen production abilities under visible light irradiation; however the hydrogen evolution rate was not stable over long time irradiation. In the case of physically mixed system of dyes and Pt- TiO_2 in TEOA aqueous, only the excited dye molecules adsorbed at the semiconductor-solution interface will contribute to the hydrogen evolution and will revert to the ground state by injecting an electron into the semiconductor and accepting an electron from TEOA, as indicated in Figure 2.12(a). On the other hands, the excited dye molecules free in the solution will change to its reduced species by accepting electron from TEOA, as shown in Figure 2.12(b), because following electron injection into Pt- TiO_2 could not take place. For the achievement of steady hydrogen evolution, a fixation of dye would be necessary to make the dyes always contacted with TiO_2 surface. Abe *et al.* (2000) investigated the chemical fixation of xanthene dyes on platinized TiO_2 particles via silane-coupling reagent with an attempt to construct a stable dye-sensitized photocatalyst system in water. It indicated that the fixation of dye via silane-coupling reagent was more stable than that via ester linkage, which is not stable in water because of hydrolysis. The Eosin Y-fixed Pt- TiO_2 exhibited steady hydrogen production from aqueous TEOA under visible light irradiation for long time, and the hydrogen evolution reproduced even after the exchange of aqueous TEOA, while the hydrogen evolution from the mixture of Eosin Y and Pt- TiO_2 ceased in 10 h. The reproducibility would indicate that the hydrogen evolution was not derived from dyes free in solution but from the dyes fixed on TiO_2 surface, and the good reproducibility was observed at least within fifth runs. Steady hydrogen evolution was achieved by the dye fixation, however the initial hydrogen evolution rate was low compared with that of the physically mixed system of Eosin Y and Pt- TiO_2 . There are the difference in hydrogen production mechanism between

the physically mixed system and the dye-fixed system. In the case of physically mixed system of xanthene dyes and Pt-TiO₂, the hydrogen production is caused by the direct electron transfer from the reduced dye to Pt metal, as well as the electron transfer through the TiO₂ conduction band. On the other hands, in the dye-fixed system, the electron transfer mainly takes place through the TiO₂ conduction band. Even though the dye-fixed system has the disadvantage that initial hydrogen generation is lower than the physically mixed system by the above-mentioned reason, it possesses several advantages, such as stability and less influence of pH.

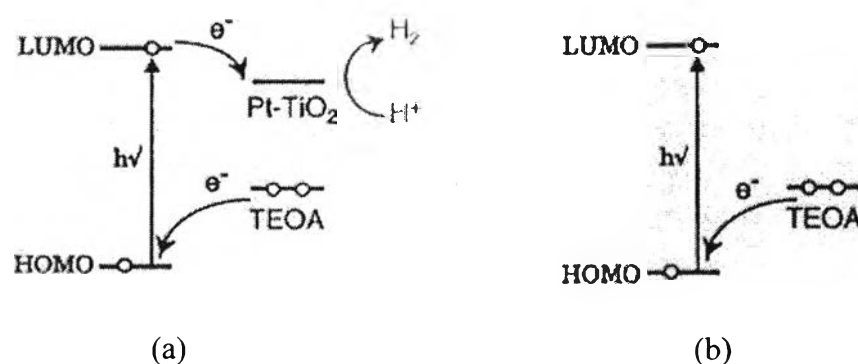


Figure 2.12 Expected photoelectron transfer on dye molecules at the solution-semiconductor interface: (a) physically mixed system of dyes and Pt-TiO₂ in aqueous TEOA and (b) dye molecules free in the TEOA solution.

Generally, the metal loading is indispensable because the metal loading influences the dye adsorption, electron transfer, and charge separation of e_{cb}^- and h_{vb}^+ (charge separation effect). These effects increase the rate of reduction of H₂O to H₂. In a previous study, the photocatalytic activities over the dye-sensitized M/TiO₂ (M = Pt, Ru, and Rh) for hydrogen production from a DEA-H₂O mixture under visible light irradiation ($\lambda > 420$ nm) was investigated in the presence of electron donors, such as triethanolamine, acetonitrile, and triethylamine (Jin *et al.*, 2006). It was found that the Eosin can be more heavily adsorbed to the metal-loaded TiO₂ by complex action than on pure TiO₂. Moreover, the number of adsorbed Eosin increased with an increase in noble metal loading significantly. Obviously, more metal loading enhanced the adsorption of Eosin, and subsequently enhanced the electron transfer and hydrogen evolution in photocatalytic reaction. In a long-term

photocatalytic reaction carried out for 100 h, the total amount of evolved hydrogen reached 32.7 ml from the DEA-H₂O aqueous solution mixture (15% v/v) over Eosin-Rh/TiO₂ (5.0 wt.%) photocatalyst. No H₂ evolution was observed over pure M/TiO₂ photocatalysts in the absence of dye under irradiation by visible light. This indicated that no direct photo-excitation of TiO₂ semiconductor had taken place.

2.6.4 Composite Semiconductors

Semiconductor composition (coupling) is another method to utilize visible light for hydrogen production. When a large band gap semiconductor is coupled with a small band gap semiconductor with a more negative CB level, CB electrons can be injected from the small band gap semiconductor to the large band gap semiconductor. Thus, a wide electron-hole separation is achieved as shown in Figure 2.13. The process is similar to dye sensitization. The difference is that electrons are injected from one semiconductor to another semiconductor, rather than from excited dye to semiconductor. Successful coupling of the two semiconductors for photocatalytic water splitting hydrogen production under visible light irradiation can be achieved when the following conditions are met: (1) semiconductors should be photocorrosion free, (2) the small band gap semiconductor should be able to be excited by visible light, (3) the CB of the small band gap semiconductor should be more negative than that of the large band gap semiconductor, (4) the CB of the large band gap semiconductor should be more negative than the reduction potential of H⁺/H₂, and (5) electron injection should be fast, as well as efficient.

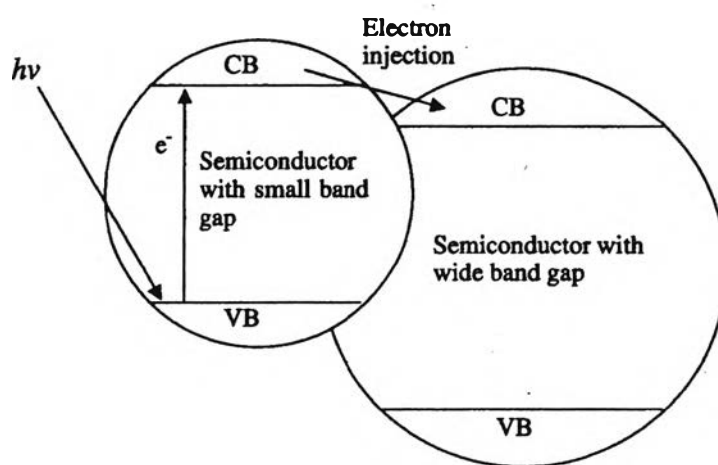


Figure 2.13 Electron injection in composite semiconductors.

It has been reported that coupling of CdS (band gap of 2.4 eV) with SnO₂ (band gap of 3.5 eV) could produce hydrogen under visible radiation (Gurunathan, 1997). Electron excited to the CB (-0.76 eV) of CdS are injected to the CB (-0.34 eV) of SnO₂ in less than 20 ps, resulting in wide electron-hole separation. Sacrificial agent, EDTA, has to be added to scavenge VB hole on CdS; otherwise, photocorrosion of CdS would occur. Doong *et al.* (2001) coupled CdS with TiO₂ for 2-chlorophenol degradation under UV irradiation. In the study, both CdS and TiO₂ could be excited. The combination of the two semiconductors showed better photocatalytic activity due to better charge separation. The CB electrons of CdS are injected to the CB of TiO₂, while the VB holes in TiO₂ are injected to the VB of CdS. Kang *et al.* (1999) employed CdS-TiO₂ composite semiconductor for 4-chlorophenol photodegradation and found that coupling of CdS with TiO₂ was more effective than CdS and TiO₂ used separately. The composite semiconductor CdS-TiO₂ can be applied to produce hydrogen since the CB of TiO₂ is more negative than hydrogen production level. So *et al.* (2004) conducted photocatalytic hydrogen production using CdS-TiO₂ composite semiconductors. Photocorrosion of CdS was prevented by addition of Na₂S. Optical absorption spectra analysis showed that CdS-TiO₂ could absorb photons with wavelength up to 520 nm. Under visible light illumination (Xe lamp), CdS-TiO₂ composite semiconductors produced hydrogen at a higher rate than CdS and TiO₂ used separately.

De *et al.* (1996) conducted solar photocatalytic hydrogen production using CdS-ZnS composite semiconductor. Photocorrosion was inhibited by addition of Na₂S/Na₂SO₃ solution. Under solar irradiation, addition of n-Si enhanced hydrogen production. This was due to the smaller band gap of n-Si together with its more negative CB. When exposed to solar radiation with wavelength longer than 520 nm, electrons were excited from the VB of n-Si to the CB of n-Si and then transferred to the CB of CdS sequentially, resulting in a higher solar radiation utilization. Similar work employing CdS-ZnS composite semiconductor for solar hydrogen production was also reported by Koca and Sahin (2002). They prepared their photocatalyst CdS-ZnS by coprecipitating of hot solutions to improve the hydrogen production rate. This may be due to better contact between CdS and ZnS particles, which could in turn improve the transfer of electrons. Besides coupling

with small band gap semiconductors, TiO_2 coupled with a large band gap semiconductor has also been investigated and proven to be more efficient under UV irradiation, as well. Nguyen *et al.* (2004) studied the effect of electronic characteristics of $\text{TiO}_2\text{-SiO}_2$ and $\text{RuS}_2/\text{TiO}_2\text{-SiO}_2$ on hydrogen production. They observed that the coupled $\text{TiO}_2\text{-SiO}_2$ semiconductor showed more negative CB than TiO_2 . When further coupled with RuS_2 , electrons could be transferred to the CB of RuS_2 (-0.6 eV), accomplishing reduction of protons to hydrogen molecules.

Tennakone and Bandara (2001) attached dye-sensitized SnO_2 nanocrystallites (10-15 nm) to platinized ZnO (about 600 nm) particles for photocatalytic hydrogen production from water, in the presence of hole scavenger (ethanol). It was found that although the CB of SnO_2 was lower (less negative) than that of ZnO, electrons from excited dyes could be transferred to ZnO via SnO_2 without relaxation to the CB energy level of SnO_2 . It was observed that electron transfer from dye to semiconductor particle (Figure 2.14) was very fast. The hydrogen production rate of the coupled Pt/ZnO/ SnO_2 /dye was found to be much higher (0.92 ml) than Pt/ZnO/dye (0.04 ml) and other combinations of these materials. Such high hydrogen production rate could be achieved by wide charge separation with SnO_2 . The successful electron transfer was possible only when the particle size of SnO_2 was small. Otherwise, electrons might be relaxed to the CB of SnO_2 , inhibiting hydrogen production. Platinum loading on the surface of ZnO was also found to be very effective for hydrogen production enhancement. It is expected that suitable coupling of different modification methods can contribute to a higher hydrogen production rate.

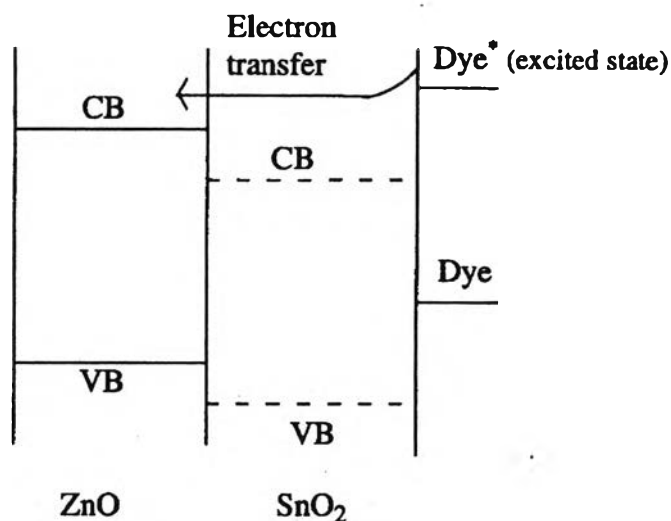


Figure 2.14 Energy level diagram indicating the band positions of SnO₂, ZnO, as well as the ground and excited state level of the dye.

Recently, Li *et al.* (2004) developed a novel photocatalyst by coupling nitrogen doping and composite semiconductors. Nitrogen-doped ZnO was coupled with WO₃, V₂O₅, and Fe₂O₃ for acetaldehyde decomposition under visible light irradiation. By doping of nitrogen, ZnO could respond with visible spectrum. Unlike coupling with WO₃ and V₂O₅, coupling with Fe₂O₃ causes the photocatalytic activity to deteriorate since Fe₂O₃ served as both an electron sink and a hole sink. Although N-doped ZnO-WO₃ and ZnO-V₂O₅ worked better under visible light irradiation for acetaldehyde decomposition, they were not suitable for hydrogen production since the CB of both WO₃ and V₂O₅ are not negative enough. It is expected that a N-doped composite semiconductor with CB level more negative than hydrogen production level, such as SiC-TiO₂, may serve as an efficient photocatalyst for hydrogen production under visible light irradiation.

2.7 Porous Material

The classification of pores according to size has been under discussion for many years, but in the past, the terms “micropore” and “macropore” have been applied in different ways by physical chemists and some other scientists. With an

attempt to clarify this situation, the limits of size of the different categories of pores included in Table 1 have been proposed by the International Union of Pure and Applied Chemistry (IUPAC) (Ishizaki et al., 1988 and Rouquerol et al., 1999). As indicated, the “pore size” is generally specified as the “pore width”, i.e. the available distance between the two opposite walls. Obviously, pore size has a precise meaning when the geometrical shape is well defined. Nevertheless, for most purposes, the limiting size is that of the smallest dimension, and this is generally taken to represent the effective pore size.

Table 2.1 Definitions about porous solids

Term	Definition
Porous solid	Solid with cavities or channels which are deeper than they are wide
Micropore	Pore of internal width less than 2 nm
Mesopore	Pore of internal width between 2 and 50 nm
Macropore	Pore of internal width greater than 50 nm
Pore size	Pore width (diameter of cylindrical pore or distance between opposite walls of slit)
Pore volume	Volume of pores determined by stated method
Surface area	Extent of total surface area determined by given method under stated conditions

According to the IUPAC classification, porous materials are regularly organized into three categories on a basis of predominant pore size as follows:

- Microporous materials (pore size < 2 nm) include amorphous silica and inorganic gel to crystalline materials, such as zeolites, aluminophosphates, gallophosphates, and related materials.

- Mesoporous materials ($2 \text{ nm} \leq \text{pore size} \leq 50 \text{ nm}$) include the M41S family (e.g. MCM-41, MCM-48, MCM-50, and etc.) and other non-silica materials synthesized via intercalation of layered materials, such as double hydroxides, metal

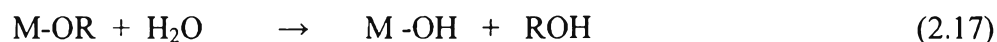
(titanium, zirconium) phosphates, and clays.

- Macroporous materials (pore size > 50 nm) include glass-related materials, aerogels, and xerogels.

Nowadays, micro- and mesoporous materials are generally called “nanoporous materials”. Particularly, mesoporous materials are remarkably very suitable for catalysis applications, whereas the pores of microporous materials may become easily plugged during catalyst preparation if high loading is sought.

2.8 Sol-Gel Process

The sol-gel process has been intensively studied because it is so effective to prepare nano-sized mesoporous materials (Sreethawong and Yosikawa, 2005). Because the perovskite oxides are also deactivated due to sintering or crystal growth during their continuous use in high temperature processes, and the catalytic performance of the perovskite oxides is well-known to depend on their specific surface area, sol-gel method presents some particular advantages through a low-temperature process, avoiding contamination of the materials. It also yields better stoichiometric control and the possibility of grain-size and grain-shape control. This technique does not require complicated instruments, such as in chemical vapor deposition method. It provides a simple and easy means of synthesizing nano-sized particles, which is essential for nano-catalysts (Wu and Lee, 2004). It involves the formation of metal-oxo-polymer network from molecular precursors, such as metal alkoxides, and subsequent polycondensation as follows:



where M = Si, Ti, Zr, Al, and R = alkyl group.

All stages, including the formation of colloid particles to form gel network, drying of wet gel, and calcination stage, can all lead to grain growth and formation of agglomerates. Hence, to carefully control the process is very essential in preparing high performance, and high reliability powders. The relative rates of hydrolysis and polycondensation strongly influence the structure and properties of the resulting

metal oxides. Typically, sol-gel-derived precipitates are amorphous in nature, requiring further heat treatment to induce crystallization. The calcination process frequently gives rise to particle agglomeration and grain growth and may induce phase transformation (Wang and Ying, 1999). Thus, a surfactant is used to prevent agglomeration of the particle. The BaTiO_3 nanoparticles synthesized by sol-gel process (Yu *et al.*, 2008) however are easy to form agglomeration. This can be avoided by the application of the surfactant, i.e. oleic acid as cheap and innocuous surfactant, thus preventing the agglomeration of particles. The sol-gel process by the addition of surfactant can help to enforce size controllability and prepare well-dispersed powders. The ideal model of forming the BaTiO_3 is shown in Figure 2.15.

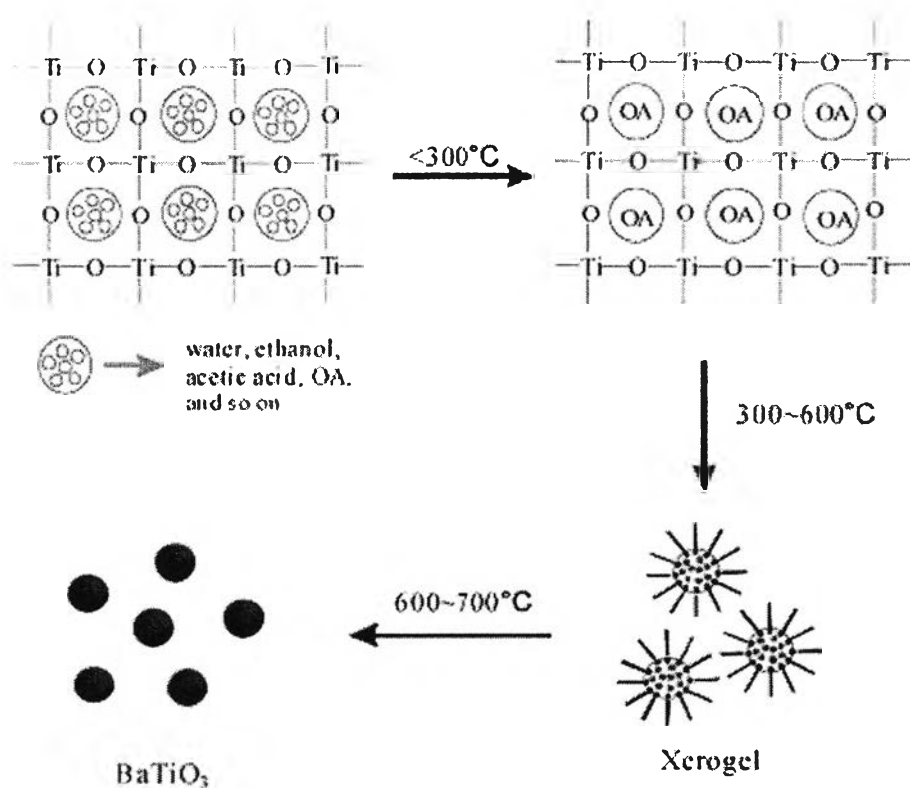


Figure 2.15 A schematic of forming the BaTiO_3 nanoparticles (Yu *et al.*, 2008).

The process can be divided to three steps. Firstly, oleic acid (OA) enmeshes in the 3D network structure of -Ti-O-Ti- when the temperature is lower than 300°C. Secondly, between 300 and 600°C, a number of “microcapsules” of BaTiO₃ precursors coated by OA are formed. The carboxyl of OA is towards the inside and hydrophobic -R group towards the outside. Excessive OA as solution will allow the system to form “micro-capsules”. Finally, when the temperature is higher than 600°C, OA decomposes, and the walls of “microcapsules” are destroyed. Although this happens, the shape of BaTiO₃ precursor is preserved, thus producing better-dispersed BaTiO₃ nanoparticles.

The mesoporous-assembled SrTiO₃ nanocrystal photocatalyst could be synthesized by a sol-gel process with the aid of structure-directing surfactant and used for photodegradation of methy orange. The different solvents resulted in different gel formation characteristics and different amounts of water required for gel formation. The use of ethanol (EtOH) as the solvent yielded a SrTiO₃ photocatalysts with a higher purity than that synthesized using ethylene glycol (EG) or the EtOH /EG mixture. The pore size distribution was found to be very narrow and monomodal when LAHC was used as a structure-directing surfactant. The mesoporous-assembled structure with a high pore uniformity of SrTiO₃ plays the most important role affecting the photocatalytic activity of the SrTiO₃ photocatalyst. The SrTiO₃ with the mesoporous-assembled structure and narrow pore size distribution synthesized at a calcination temperature of 700°C, a heating rate of 1°C/min, a LAHC-to-TIPT molar ratio of 0.25:1, and using an EtOH solvent provided the highest photocatalytic degradation activity, which was much higher than that of the non-mesoporous-structured commercial SrTiO₃ (Puangpetch, *et al.*, 2008).